



Published in final edited form as:

*Neuroimage*. 2013 March ; 68: 154–161. doi:10.1016/j.neuroimage.2012.11.052.

## Prospective active marker motion correction improves statistical power in BOLD fMRI

Jordan Muraskin<sup>a</sup>, Melvyn B. Ooi<sup>b</sup>, Robin I. Goldman<sup>a</sup>, Sascha Krueger<sup>c</sup>, William J. Thomas<sup>a</sup>, Paul Sajda<sup>a</sup>, and Truman R. Brown<sup>d</sup>

Jordan Muraskin: jsm2112@columbia.edu; Melvyn B. Ooi: mbooi@stanford.edu; Robin I. Goldman: rg2146@columbia.edu; Sascha Krueger: sascha.krueger@philips.com; William J. Thomas: billthomas2020@gmail.com; Paul Sajda: ps629@columbia.edu; Truman R. Brown: brotrr@muscc.edu

<sup>a</sup>Department of Biomedical Engineering, Columbia University, 351 Engineering Terrace, 1210 Amsterdam Avenue, New York, NY, USA 10027

<sup>b</sup>Department of Radiology, Stanford University, Lucas Center, 1201 Welch Road, Stanford, CA, USA 94305

<sup>c</sup>Philips Research Hamburg, Röntgenstrasse 24-26, 22335 Hamburg, Germany

<sup>d</sup>Department of Radiology, Medical University of South Carolina, PO Box 250322, 169 Ashley Avenue, Charleston, SC, USA 29425

### Abstract

Group level statistical maps of blood oxygenation level dependent (BOLD) signals acquired using functional magnetic resonance imaging (fMRI) have become a basic measurement for much of systems, cognitive and social neuroscience. A challenge in making inferences from these statistical maps is the noise and potential confounds that arise from the head motion that occurs within and between acquisition volumes. This motion results in the scan plane being misaligned during acquisition, ultimately leading to reduced statistical power when maps are constructed at the group level. In most cases, an attempt is made to correct for this motion through the use of retrospective analysis methods. In this paper, we use a prospective active marker motion correction (PRAMMO) system that uses radio frequency markers for real-time tracking of motion, enabling on-line slice plane correction. We show that the statistical power of the activation maps is substantially increased using PRAMMO compared to conventional retrospective correction. Analysis of our results indicates that the PRAMMO acquisition reduces the variance without decreasing the signal component of the BOLD (beta). Using PRAMMO could thus improve the overall statistical power of fMRI based BOLD measurements, leading to stronger inferences of the nature of processing in the human brain.

### Keywords

active tracking; radio-frequency markers; echo planar imaging; fMRI; group analysis; prospective motion correction

---

© 2012 Elsevier Inc. All rights reserved.

Correspondence to: Jordan Muraskin, jsm2112@columbia.edu.

**Publisher's Disclaimer:** This is a PDF file of an unedited manuscript that has been accepted for publication. As a service to our customers we are providing this early version of the manuscript. The manuscript will undergo copyediting, typesetting, and review of the resulting proof before it is published in its final citable form. Please note that during the production process errors may be discovered which could affect the content, and all legal disclaimers that apply to the journal pertain.

## 1. Introduction

Functional magnetic resonance imaging (fMRI), which exploits the blood oxygen level dependent (BOLD) signal, is among the most widely used tools in cognitive neuroscience and neurobiology and has recently been adopted as a clinical modality for detecting, assessing and tracking functional changes in neurological disease [28,34,45,49,6]. fMRI provides a non-invasive and relatively high spatial resolution (2–3 mm in-plane) method for observing functional activity from the entire brain volume. It is used not only to investigate task-related changes in hemodynamics [26], but also to probe brain networks [4,2,15,20,37,29] and hemodynamic correlates of other neural measures [19,50,40] during functional tasks, at rest, and during sleep [44,5,1].

The BOLD signal in fMRI is most commonly captured with echo planar imaging (EPI) sequences, which allow for the rapid acquisition of whole brain volumes on a slice-by-slice basis at closely sampled time-points; an acquisition of the entire brain volume requires approximately 2 seconds. Typically, the BOLD signal of interest is very small (1–5%) relative to the overall measured signal variability [38]. Therefore, data analysis relies on statistical methods that integrate information over multiple acquisition volumes, making them extremely sensitive to head motion during the experimental protocol. Even small head movements during acquisition can reduce BOLD signal sensitivity, for example by causing partial volume mixing effects due to the relative slice alignment changing during acquisition, resulting in fluctuations in signal intensity comparable to the signal of interest itself. These motion artifacts lead to inaccurate and poor quality activation maps [21,24,18,16]. While all subject populations are susceptible to motion artifacts, these problems are likely to be exacerbated in clinical fMRI studies, as patients are more likely to move than healthy volunteers [24,18,39,43,3].

To correct for head motion, fMRI studies typically use retrospective image analysis techniques, most commonly FSL's MCFLIRT [22] and SPM's SPM\_REALIGN [17]. These algorithms estimate the parameters of the six degrees of freedom (6-df) transformation of a rigid body movement by assuming the sequentially measured brain slices that make up a volume are a single rigid object, and use these parameters to align all the slices in each volume in the data time series identically after image acquisition. Retrospective alignment methods rely on interpolation schemes, which can blur the data and, further, cannot fully account for the effects of through-plane motion and local spin history effects [18]. Also, these techniques commonly compensate for inter-volume movements, but neglect intra-volume movement between slices [30]. If subject motion occurs during acquisition of a brain volume, slices within that volume would be captured at different angles and/or spacing lengths violating the assumption of rigid body motion on which these techniques rely. Recently, a number of prospective realignment techniques have been developed that attempt to keep constant the scan plane orientation and position with respect to the head, throughout the acquisition. These methods aim to track the 6-df motions and correct the acquisition online. Broadly speaking they can be classified into image-based methods [46] which can only correct for inter-volume movements, navigator-based methods [11], which acquire extra data along various three-dimensional k-space trajectories to estimate the 6-df [35,51,52,48,53], and marker-based methods which follow in real time the position of external markers attached to the head either by optical tracking [54,42,36,14,27] or using MRI [10,55,13,12,25,7,31,32]. Our group has developed prospective active-marker motion correction (PRAMMO) for structural [31] and echo-planar brain scans and demonstrated potential advantages of the approach for functional imaging [32,33]. However, our initial experiments were done assuming substantial and highly controlled motion as well as results reported for individual subjects.

Since most fMRI studies report results at the group level (across a subject population) the true utility of prospective correction methods must be demonstrated across a more representative population size, with realistic task paradigms and natural experimental conditions. So far no study has investigated the effects of prospective active marker real time motion correction in this way, and therefore it is difficult to determine if the extra cost and inconvenience of using a prospective system is justified by a resulting improvement in data quality and statistical power. Here we assess, *in vivo*, the difference in statistical power provided by PRAMMO versus conventionally used retrospective techniques for three well-established visual and motor paradigms in a realistic acquisition situation. We report the statistical effects of PRAMMO correction in fMRI at the group level, showing it substantially increases both the size and significance of the activated regions in all the paradigms. We further show that most of the improvement in the statistical power arises from a small increase in effect size and reduction in variance.

## 2. Methods and Materials

### 1. Active Marker Tracking Device and Scan-Plane Update

Details of the tracking hardware and scan-plane update scheme have been previously presented [31,32] and are briefly reviewed here. Motion tracking was performed using three active markers integrated into a rigid plastic headband worn by the volunteer. Three markers in 3D space are sufficient to fully describe any arbitrary rigid-body head motion. Each marker is a solenoid inductor, tuned and matched to 64.3 MHz, containing a small glass sphere (3 mm diameter) filled with Gd-doped water solution. The markers are attached to a Synergy Multi-Connect box (Philips Healthcare, Best, the Netherlands; by IGC Medical Advances), which then connects to the scanner (see ref. [31], Fig. 1).

Real-time, slice-by-slice prospective correction in a single-shot EPI scan is achieved by interleaving a rapid track-and-update module into the imaging sequence before the acquisition of each EPI-slice (see ref. [32], Fig. 1). The tracking module contains a short tracking pulse-sequence of orthogonal one-dimensional projection-readouts that measures the three-dimensional positions of the active markers. Because the markers are on separate receive channels, they are measured simultaneously and unambiguously identified. The spherical samples are excited by a weak, nonselective RF-pulse (Flip Angle=4/degree) from the volume coil, minimizing the effects on imaged spins. A peak search and quadratic fit in frequency is used to estimate each marker's position along the projected axis. Previous studies have demonstrated measurement precision and accuracy with this method to be 0.01 and 0.3 mm, respectively [32].

In the update module for every slice acquisition, the current marker positions are compared with their initial reference positions (measured by the first tracking module at the beginning of the scan), and the 6-df rigid-body transform (three rotations  $\theta_x$ ,  $\theta_y$ ,  $\theta_z$  and three translations  $t_x$ ,  $t_y$ ,  $t_z$ , given in the image coordinate-system) is calculated [47]. The transform is then fed back to prospectively update the scan-plane of the next slice for rotational and translational head motion-by dynamically modifying the relevant imaging RF, gradient, and data acquisition attributes-before the subsequent EPI readout. The total time for each track-and-update is  $\approx 25$  msec.

### 2. Subjects

Fourteen healthy subjects (3 female, ages 21–55) participated in this study. Two data sets were discarded due to hardware malfunctions during the exam making our final  $n=12$ . Volunteers were asked to remain motionless for all scans, as they would be during a typical functional imaging protocol. The Columbia University Institutional Review Board (IRB) approved all experiments and informed consent was obtained before each exam.

### 3. Paradigms

Prospective active marker motion (PRAMMO) correction was evaluated using three well-established block design paradigms: Flickering checkerboard (FC), Face localizer (FL), and Finger tapping (FT). For all the tasks, a block design that alternated between “control” and “stimuli” was presented. For the FC paradigm, stimuli blocks of 15s displaying a checkerboard flashing at 7Hz were interleaved with 15s fixation cross control blocks. The stimuli blocks were repeated five times for a scan time of 175s. In the FL paradigm, subjects were passively shown faces at a rate of 1Hz for blocks of 20s interleaved with blocks of isointense Gaussian random noise images presented at the same rate. The blocks were repeated six times for a scan time of 265s. For the FT paradigm, the subject responded to the text “TAP!” by tapping his/her right fingers until “REST” was displayed. These blocks were each 15s and were repeated 5 times for a scan time of 180s.

In each paradigm, two scans of PRAMMO “on” and two scans of PRAMMO “off” were acquired in a random order blinded to the subject. For scans with correction “off,” all tracking and geometry calculations were performed and logged but were not applied to update the scan plane. A single TTL pulse sent from the scanner, at the start of the scan, to the presentation computer provided precise timing control of the paradigm runs.

### 4. Data Acquisition

Experiments were performed on a 1.5-T Philips Achieva (Philips Healthcare, Best, The Netherlands). Imaging was performed with a standard quadrature birdcage coil, and tracking via active-marker headband. Slice-by-slice prospective correction (tracking parameters: TE/TR = 1.8/4.3 ms, FA = 4 degrees, resolution = 1 mm, rejection threshold = 10 mm) was applied to an axial, single-shot two-dimensional-EPI time series (imaging parameters: TE/TR = 40/1680 ms, FA = 80 degrees, FOV = 220 × 220 mm, voxel size = 3 × 3 mm, thickness/ gap = 5/1 mm, slices = 13, phase-encode direction = right-left, shim = first-order [subject-specific], 76 repetitions for FC, 115 for FL, and 78 for FT).

Images were reconstructed using the scanner’s standard processing pipeline. Scan durations increased due to extensive real-time logging of tracking information required at this developmental stage, increasing the effective TR to 2.3s. Instead of full brain coverage with longer TRs, we chose to increase the number of repetitions by reducing the number of slices per volume. With logging disabled, scan duration is reduced by ≈27%. A single EPI scan with 25 slices was acquired to help in registration along with a T1-weighted structural 3D-MPRAGE (TE/TR/TI/shot interval= 4 ms/ 8.3 ms/1000 ms/1500 ms, FA= 8°, FOV=240 × 240 × 150 mm, voxel size = 1.25 × 1.25 × 2 mm, slices = 125, ETL =48, scan time=6:50 min:s). Respiration measures were taken for nine of the subjects using the scanner’s respiratory bellows monitor (Philips Healthcare, Best, The Netherlands) and continuously sampled at 500Hz throughout each scan.

### 5. fMRI preprocessing and analysis

To investigate the advantages of PRAMMO over standard retrospective motion correction techniques (e.g. as provided in SPM and FSL), we performed a general linear model (GLM) analysis using the FMRIB software library [41]. All fMRI data, both PRAMMO “on” and “off”, was pre-processed with the following: brain extraction, spatial smoothing using a Gaussian kernel of 5mm FWHM, and high-pass filtering with the high-pass cutoff at 100s. PRAMMO “off” scans were sent through three separate analysis pipelines: 1) retrospectively motion corrected using MCFLIRT [41], 2) retrospectively motion corrected using SPM\_REALIGN (Statistical Parametric Mapping v8 (SPM8), Well come Trust, London, UK) and 3) no motion correction. Retrospective motion correction was not applied to PRAMMO “on” scans. Since the block design of the fMRI paradigm makes slice-time

correction unneeded we did not use it in most of our analysis although, to confirm it did not affect the comparison of PRAMMO “on” to “off” (because it mixes space and time domains), a complete analysis of each paradigm was run using it. The full three-level (scan, subject, and group) fMRI analysis was run separately for each experiment and motion correction technique. Thus, 4 group level mixed-effects results were obtained for each functional paradigm, one from the PRAMMO “on” data and three from the PRAMMO “off” data. At each level, activated regions that passed a corrected cluster threshold of  $p < 0.05$  at a z-score threshold of 2.3 were considered significant.

In addition to the standard group mean for each motion correction technique, we ran three fixed-effects paired t-tests at the subject level to compare PRAMMO with each retrospective correction technique-PRAMMO “on” to 1) PRAMMO “off” with MCFLIRT correction, 2) PRAMMO “off” with SPM\_REALIGN correction, and 3) PRAMMO “off” with no motion correction. Activated regions were considered significant if they passed a voxel threshold of  $p < 0.001$  (uncorrected). In a second analysis to explore the advantages of PRAMMO at the subject level, a region of interest analysis was used to compare subject level mean z-scores and mean beta and variance changes from baseline. To create the ROIs for all three experimental paradigms, each motion correction technique’s group level activation maps were thresholded at  $p < 0.001$ . The intersection of activated voxels across all four techniques was used as the paradigm’s region of interest. For each subject and motion correction technique, the means of the z-scores, beta and variance percent signal change from baseline within the paradigm’s ROI were calculated. A paired Wilcoxon Signed Rank test collapsed across experimental paradigms was used to determine significant within-subject differences between PRAMMO and retrospective motion correction techniques for z-scores, beta and variance signal changes.

We also compared the subject motion recorded by the active markers between the “on” and “off” trials. The mean RMS displacement as well as the mean relative (repetition-to-repetition) RMS displacement was calculated for each trial. A group student’s t-test on the motion data in total and within each paradigm was used to make sure the subjects’ movements were comparable.

### 3. Results

#### 1. Motion Tracking

All group Students’ t-tests on the motion data indicate that the amount of motion was not significantly different for all PRAMMO “on” (0.24 +/- 0.17 mm) and “off” (0.27 +/- 0.20 mm) scans ( $p = 0.26$  two-tailed Student’s t-test). There was also no difference between “on” and “off” within paradigms ( $p = 0.85$  for FC,  $p = 0.13$  for FL, and  $p = 0.86$  for FT). Even though subjects were instructed to remain still throughout the scan, small head drifts and respiratory movements were common in the data. An example motion plot for a single scan is shown in Fig. 1A as well as a finer temporal resolution of the same plot in Fig. S1.

To assess the performance of all the motion correction techniques, linear correlations of the mean absolute root mean squared (RMS) motion measurements (PRAMMO) and estimates (FSL, SPM) for both the PRAMMO “on” and “off” scans are plotted in Fig. 1B. The linear correlation between PRAMMO measurements and FSL estimates in the PRAMMO “off” case is displayed as the blue fit ( $R^2 = 0.76$ ) while the correlation between PRAMMO measurements and SPM estimates is the red fit ( $R^2 = 0.74$ ). In the PRAMMO “on” case, the green and cyan fits are the correlations between PRAMMO measurements and FSL estimates ( $R^2 = 0.38$ ) and PRAMMO measurements and SPM estimates ( $R^2 = 0.26$ ), respectively. As expected, the FSL and SPM estimates were approximately equal to each other for both the “on” and “off” cases but showed less of a relationship to the PRAMMO

corrected motions in the “on” case. The mean estimated motions for PRAMMO “on” scans by FSL and SPM were  $0.10 \pm 0.05$  mm and  $0.12 \pm 0.06$  mm. The motion estimates from FSL and SPM only accounted for approximately 75% of the measured motion in the “off” case (*slopes* =  $0.74 \pm 0.10$  and  $0.76 \pm 0.11$  95% CI respectively).

## 2. Subject Level and Traditional Group GLM of Motion Correction Data

At the single-subject level, each task elicited a strong BOLD response in task-related areas, which is shown for a single voxel in the raw and smoothed data (Fig. 2, Fig. S2). At the group level, brain regions that passed the cluster threshold for each experimental paradigm and motion correction technique are displayed in Fig. 3. The columns represent different motion correction techniques, while the rows are the different experimental paradigms. The locations of activation are consistent across techniques and appear in the expected regions for each paradigm: large activations in the occipital lobe and visual cortex for FC, predominately right-sided Fusiform Face Area (FFA) and Lateral Occipital Cortex (LOC) for FL, and left primary motor cortex for FT. Data corrected with PRAMMO (PRAMMO “on”) consistently had larger cluster sizes and higher mean cluster z-scores than the other motion correction methods. Cluster sizes (wide bars) and mean z-scores (thin bars) for each paradigm and correction technique are reported in Fig. 4. No significant difference in the results was observed when slice-timing correction was carried out (data not shown).

## 3. Voxel-wise Paired t-test

Fig. 5 shows voxels where the PRAMMO “on” datasets have statistically higher activations compared to PRAMMO “off” corrected with FSL, SPM, and when no retrospective motion correction technique is applied. The columns represent different motion correction techniques, while the rows are the different experimental paradigms. Areas of increased statistical significance ( $p < 0.001$  uncorrected) are located in the same areas as those found using the traditional group general linear model (GLM). PRAMMO increased statistical significance in the occipital lobe and visual cortex for FC paradigm and in the bilateral FFA as well as LOC for FL paradigm. No significant difference was seen for the FT paradigm.

## 4. Region of Interest Analysis

The paradigm’s regions of interest were quite large, encompassing volumes of 26.6 cc(3320 voxels) for FC, 5.7 cc(708 voxels) for FL, and 7.7cc(963 voxels) for FT. Mean z-scores and percent signal change from baseline for Beta and Variance are plotted in Fig. 6. Bars represent mean across all three experimental paradigms. A two-tailed paired Wilcoxon Signed Rank test was used to determine significant differences between PRAMMO and the two retrospective as well as the no correction techniques. An “\*” indicates that technique’s mean is significantly different from PRAMMO at the  $p < 0.05$  level. The ROI analysis shows PRAMMO has higher mean z-scores and Betas than all three other techniques, and lower (no correction) or similar (FSL, SPM) Variance.

## 4. Discussion

This paper demonstrates that our prospective active marker motion correction system, PRAMMO, provides significantly higher quality activation maps compared to standard retrospective motion correction techniques during three common fMRI experiments. Not only did our system provide larger activation areas but also statistically significant increases in z-scores for activated regions at the group level which appeared to be due to both a small increase in  $\beta$ -values and a decrease in the residuals of the individual subject GLM fits. Most studies have analyzed their prospective motion correction systems for fMRI by calculating a quality metric of images taken with the prospective correction “on” and comparing it with the correction “off” for cases with and without motion [35,51,52,48,54,42]. Our previous

study analyzed PRAMMO not only by a quality metric but also by simulating an fMRI experiment, which showed PRAMMO increased statistical significance in activated regions of interest over retrospective techniques in the “deliberate motion” case [32]. We subsequently confirmed these results in an actual fMRI experiment involving a breath-holding task [33]. One study by Speck et al. showed that their optical correction system increases the number of activated voxels while decreasing both false positives and false negatives in an *in-vivo* visual fMRI paradigm [42]. However, this study involved exaggerated  $\pm 15$  degrees rotation every 10 seconds, and a small sample size ( $n=2$ ). In our present study, the subjects’ heads were not fixed although they were instructed to keep as still as possible which still allowed for free motion during the scans. Using the positions of the active marker, we showed that the type and range of movement was consistent across scans and subjects and within the range of a typical fMRI experiment ( $< 1$  mm RMS displacement). After retrospective correction, we compared the FSL and SPM\_REALIGN algorithm’s motion estimates to PRAMMO’s active marker measurements. The high coefficients of determination for FSL ( $R^2= 0.74$ ) and SPM ( $R^2= 0.76$ ) indicate good agreement with PRAMMO. However, there is a discrepancy of  $\approx 25\%$  between the measured motion and estimated motion for both FSL and SPM. The reduction in accuracy could be due to image blurring and slice misalignment during acquisition when movement is present. Interestingly, both algorithms assessed their accuracies by taking motion estimates and applying the 6-df transforms to sample datasets and running their motion correction techniques [18,22] with reported accuracies of  $\approx 0.1$  mm. However, the algorithms can only process inter-volume registrations, and thus intra-volume movements, which in effect change the shape of the imaged brain from volume to volume, may affect the algorithms’ accuracies when compared to PRAMMO. It has been previously shown using an MRI simulator that continuous motion during an EPI time series can increase the RMS error of parameter estimation by a factor of 1.7 [8,9]. To confirm that we are seeing an underestimation by FSL and SPM and not an overestimation by our tracking coils, we replicated the results of Drobjnak et al. with both synthetic and PRAMMO recorded motion data (Fig. S5–S9). FSL consistently underestimates the amount of motion similar to our real data. Further experiments are need to confirm, but our results indicate that we may be observing a true underestimation of motion by retrospective techniques with real data.

For runs when PRAMMO is on, and thus the subject motion is being corrected in real-time, the coefficients of determination are smaller ( $R^2= 0.38$  for FSL and  $R^2= 0.26$  for SPM), suggesting that the retrospective algorithms are modeling noise in the images instead of motion since the motion has been effectively removed. As a further validation of the success of the PRAMMO feedback, the estimated error for both FSL and SPM motion correction routines (the vertical spread of the PRAMMO on points in Fig. 1B) is approximately 0.1 mm, the same value reported for the accuracy of these routines. This strongly suggests that the underlying data represents an unmoving head since if there were extra motion it should increase the expected variance.

For each paradigm, group level fMRI maps using PRAMMO either had larger clusters and/or higher mean z-scores than those using the retrospective correction techniques. In the FC paradigm, the PRAMMO map’s activation size was over 10% larger that of FSL, SPM and the no correction analysis. The FL and FT paradigm showed similar results. Also, only PRAMMO preserved the cluster in the Supplementary Motor Cortex for the Finger Tapping experiment. This highlights PRAMMO’s effect on improving statistics in areas close to a tissue/CSF or tissue/air boundary, such as the FFA or orbito-frontal regions of the brain, where small through-plane motions can have a larger impact on signal degradation. The PRAMMO cluster also covers more of the inferior part of the post-central gyrus compared to all the other techniques for the FT paradigm. These increases in size of the activated

regions are consistent with Speck et al, who have also described significant increases in activation in a visual paradigm with their optical system [42].

While the group activation maps show PRAMMO's ability to increase cluster size at the group level, the reason for this improvement is not entirely clear due to the mixed-effects model. To investigate this further, we ran both a Voxel-wise paired t-test and a Region of Interest analysis to determine how and in what areas PRAMMO produces better activations. The paired t-test indicates that within subjects, PRAMMO has higher activations at the center of the clusters (Fig. 5).

Also, an ROI approach was used to further investigate within-subject differences. We showed that PRAMMO significantly increases mean z-scores across large ROIs and paradigms. FSL and SPM have reduced z-scores compared to PRAMMO because the blurring caused by interpolation during retrospective correction reduces FSL and SPM's beta estimates. Both algorithms reduce the variance compared to no retrospective correction; however, PRAMMO reduces the variance without lowering the beta estimate and therefore maintains higher z-scores (Fig. 6). PRAMMO significantly increases z-scores compared to no retrospective correction by lowering both the GLM variance (two-sided paired Wilcoxon Signed Rank test,  $p=0.07$ ) and by slightly increasing the beta estimate (two-sided paired Wilcoxon Signed Rank test,  $p=0.12$ ). Previous prospective motion correction studies with fMRI paradigms [42,51] attribute their improved results to a drop in variance. However, this claim was never investigated or shown with experiments.

Gaussian smoothing creates another potential confound in this analysis. The smoothing links the spatial extent and amplitude so as to make it difficult to decipher whether PRAMMO has larger clusters in the group results because of higher amplitude at the center or if PRAMMO increases signal and decreases variance in a larger area. To address this concern, we reran the entire subject and group analysis without smoothing and instead of using Family-Wise Error Correction (which requires a smoothness estimate), we used False Discovery Rate to correct for multiple comparisons. Similar to the smoothed results, at the subject level PRAMMO slightly increases the number of voxels that pass threshold (Fig. S3). To compare to the smoothed dataset's group results, we ran the group level mixed effects analysis with FDR correction (Fig. S4). These results indicate that the increase in cluster size at the group level is due to an increase in signal and decrease in variance across a large area and not just at the center of the clusters.

Presumably, PRAMMO creates higher quality activation maps by updating the image axis with every slice acquisition, which reduces the volume of spins with incorrect spin-excitation history entering the imaging plane by keeping the scan orientation the same for each measurement and also by removing the blurring caused by interpolation during retrospective correction. Using PRAMMO, the captured brain volume is a true rigid body, and thus the assumption of fMRI image analysis—that each voxel represents the identical brain region across the data time series—holds true.

A potential drawback of our experimental design was that each paradigm had only two scans for PRAMMO “on” and “off”. This may allow for one “on” or “off” scan in which the subject was not paying as much attention to bias the results. However, we don't believe this to be a serious issue as the subject was blinded to when PRAMMO was “on” or “off” and the data is consistent across a large number of subjects and paradigms.

Since in fMRI the temporal sampling of the brain volume is slow (e.g TR 2–3 s) relative to the frequency of significant movement by the subject, methods which enable both inter and intra volume correction offer the most potential to improve SNR and sensitivity of hypothesis testing. The results we report here thus demonstrate that inter and intra volume

correction via real-time tracking of active-markers increases sensitivity to BOLD signal changes so as to substantially improve statistical power at the group level.

## 5. Conclusion

In summary, we have shown that PRAMMO significantly increases the spatial extent and/or mean statistical significance of task-specific BOLD signals acquired in fMRI studies having typical amounts of subject motion. Our results are consistent with previous research [42,32] but have further demonstrated the utility of the technique via increasing the number of subjects and showing that prospective motion correction not only improves individual subject data, but also statistically improves fMRI results at the group level, relative to commonly used retrospective techniques. Given that this increase was found for motion under half a voxel in size, our results show that PRAMMO could have a significant impact for fMRI studies with even the most compliant (e.g. minimal motion) subjects. Our earlier work [32,33] has shown that PRAMMO is effective for larger amplitude motion as well, and thus, is useful for imaging less compliant subjects, challenging clinical or pediatric populations, or states such as sleep where motion over time may become problematic. As our prospective active marker correction can be implemented with relatively minor changes to hardware and software and can be added to any clinical or research scanner with multi-channel capability, PRAMMO would be feasible for use in most clinical or research settings. It should be noted as well that PRAMMO can be added to other functional sequences such as connectivity mapping or arterial spin labeling (ASL), spectroscopic imaging, tract mapping such as diffusion tensor imaging (DTI), or other anatomical sequences to minimize the effects of motion on data quality for these types of images as well. Thus, as PRAMMO improves fMRI data significance at both the individual and group level, it may facilitate imaging of challenging subjects or populations who may otherwise not be able to be adequately imaged. And, as it can easily be added to a multitude of data acquisition paradigms, PRAMMO could have wide impact on both neuroscientific and clinical functional as well as anatomical imaging.

## Supplementary Material

Refer to Web version on PubMed Central for supplementary material.

## Acknowledgments

This work has been supported by NIH R21EB006877, NIH/NCRR UL1RR024156, and NIH R01MH085092. We would like to thank Stephen Dashnaw and Glenn Castillo for their help in this project. We would also like to thank the two anonymous reviewers who have greatly contributed to making this manuscript significantly better.

## References

1. Andrade KC, et al. Sleep spindles and hippocampal functional connectivity in human NREM sleep. *J Neurosci*. 2011; 31(28):10331–10339. [PubMed: 21753010]
2. Biswal BB, et al. Toward discovery science of human brain function. *Proc Natl Acad Sci U S A*. 2010; 107:4734–4739. [PubMed: 20176931]
3. Brown TT, et al. Prospective motion correction of high-resolution magnetic resonance imaging data in children. *NeuroImage*. 2010; 53:139–145. [PubMed: 20542120]
4. Calhoun VD, Maciejewski PK, Pearlson GD, Kiehl KA. Temporal lobe and “default” hemodynamic brain modes discriminate between schizophrenia and bipolar disorder. *Human Brain Map*. 2008; 29(1):1265–1275.
5. Dang-Vu TT, et al. Spontaneous neural activity during human slow wave sleep. *Proc Natl Acad Sci U S A*. 2008; 30;105(39):15160–15165.

6. deCharms RC, et al. Control over brain activation and pain learned by using real-time functional MRI. *Proc Natl Acad Sci U S A*. 2005; 102(51):18626–18631. [PubMed: 16352728]
7. Derbyshire JA, Wright GA, Henkelman RM, Hinks RS. Dynamic scanplane tracking using MR position monitoring. *J Magn Reson Imaging*. 1998; 8:924–932. [PubMed: 9702895]
8. Drobnjak I, Gavaghan D, Suli E, Pitt-Francis J, Jenkinson M. Development of a functional magnetic resonance imaging simulator for modeling realistic rigid-body motion artifacts. *Magn Reson Med*. 2006; 56:364–380. [PubMed: 16841304]
9. Drobnjak I, Pell GS, Jenkinson M. Simulating the effects of time-varying magnetic fields with a realistic simulated scanner. *Magn Reson Imaging*. 2010; 28:1014–1021. [PubMed: 20418038]
10. Dumoulin CL, Souza SP, Darrow RD. Real-time position monitoring of invasive devices using magnetic resonance. *Magn Reson Med*. 1993; 29:411–415. [PubMed: 8450752]
11. Ehman RL, Felmlee JP. Adaptive technique for high-definition MR imaging of moving structures. *Radiology*. 1989; 173:255–263. [PubMed: 2781017]
12. Elgort DR, et al. Real-time catheter tracking and adaptive imaging. *J Magn Reson Imaging*. 2003; 18:621–626. [PubMed: 14579407]
13. Flask C, et al. A method for fast 3D tracking using tuned fiducial markers and a limited projection reconstruction FISP (LPR-FISP) sequence. *J Magn Reson Imaging*. 2001; 14:617–627. [PubMed: 11747015]
14. Forman C, Aksoy M, Hornegger J, Bammer R. Self-encoded marker for optical prospective head motion correction in MRI. *Med Image Comput Comput Assist Interv*. 2010; 13(pt 1):259–266. [PubMed: 20879239]
15. Fox MD, Greicius MD. Clinical applications of resting state functional connectivity. *Front Syst Neurosci*. 2010; 4:19. [PubMed: 20592951]
16. Freire L, Mangin JF. Motion correction algorithms may create spurious brain activations in the absence of subject motion. *NeuroImage*. 2001; 14:709–722. [PubMed: 11506543]
17. Friston KJ, et al. Spatial registration and normalization of images. *Hum Brain Map*. 1995; 2:165–189.
18. Friston KJ, Williams S, Howard R, Frackowiak RS, Turner R. Movement-related effects in fMRI time-series. *Magn Reson Med*. 1996; 35:346–355. [PubMed: 8699946]
19. Goldman RI, et al. Single-trial discrimination for integrating simultaneous EEG and fMRI: identifying cortical areas contributing to trial-to-trial variability in the auditory oddball task. *NeuroImage*. 2009; 47:136–47. [PubMed: 19345734]
20. Greicius MD, Krasnow B, Reiss AL, Menon V. Functional connectivity in the resting brain: a network analysis of the default mode hypothesis. *Proc Natl Acad Sci U S A*. 2003; 100:253–258. [PubMed: 12506194]
21. Hajnal JV, et al. Artifacts due to stimulus correlated motion in functional imaging of the brain. *Magn Reson Med*. 1994; 31:283–291. [PubMed: 8057799]
22. Jenkinson M, Bannister PR, Brady JM, Smith SM. Improved optimisation for the robust and accurate linear registration and motion correction of brain images. *NeuroImage*. 2002; 17(2):825–841. [PubMed: 12377157]
23. Kanwisher N, McDermott J, Chun MM. The Fusiform Face Area : A Module in Human Extrastriate Cortex Specialized for Face Perception. *NeuroImage*. 1997; 17(11):4302–4311.
24. Krings T, et al. Functional MRI for presurgical planning: problems, artefacts, and solution strategies. *J Neurol Neurosurg Psychiatry*. 2001; 70:749–760. [PubMed: 11385009]
25. Krueger, et al. Fast and accurate automatic registration for MR-guided procedures using active microcoils. *IEEE Trans Med Imaging*. 2007; 26:385–392. [PubMed: 17354643]
26. Kwong KK, et al. Dynamic magnetic resonance imaging of human brain activity during primary sensory stimulation. *Proc Nat Acad Sci U S A*. 1992; 89:5675–5679.
27. Lerner T, Rivlin E, Gur M. Vision-Based Tracking System for Head Motion Correction in FMRI Images. *Advances in Computer Graphics and Computer Vision*. 2007:381–394.
28. Matthews PM, Honey GD, Bullmore ET. Applications of fMRI in translational medicine and clinical practice. *Nat Rev Neurosc*. 2006; 7:732–744.

29. Negishi M, Martuzzi R, Novotny EJ, Spencer DD, Constable RT. Functional MRI connectivity as a predictor of the surgical outcome of epilepsy. *Epilepsia*. 2011; 52(9):1733–1740. [PubMed: 21801165]
30. Oakes TR, et al. Comparison of fMRI motion correction software tools. *NeuroImage*. 2005; 28(3): 529–543. [PubMed: 16099178]
31. Ooi MB, Krueger S, Thomas WJ, Swaminathan SV, Brown TR. Prospective real-time correction for arbitrary head motion using active markers. *Magn Reson Med*. 2009; 62:943–954. [PubMed: 19488989]
32. Ooi MB, Krueger S, Muraskin J, Thomas WJ, Brown TR. Echo-planar imaging with prospective slice-by-slice motion correction using active markers. *Magn Reson Med*. 2011; 66:73–81. [PubMed: 21695720]
33. Ooi MB, et al. Combined prospective and retrospective correction to reduce motion-induced image misalignment and geometric distortions in EPI. *Magn Reson Med*. 2012 epub.
34. Owen AM, Coleman MR. Functional neuroimaging of the vegetative state. *Nat Rev Neurosc*. 2008; 9(3):235–243.
35. Pipe JG. Motion correction with PROPELLER MRI: application to head motion and free-breathing cardiac imaging. *Magn Reson Med*. 1999; 42:963–969. [PubMed: 10542356]
36. Qin L, et al. Prospective head-movement correction for high-resolution MRI using an in-bore optical tracking system. *Magn Reson Med*. 2009; 62:924–934. [PubMed: 19526503]
37. Raichle ME, et al. A default mode of brain function. *Proc Natl Acad Sci U S A*. 2001; 98:676–682. [PubMed: 11209064]
38. Ramsey NF, et al. Functional Mapping of Human Sensorimotor Cortex with 3D BOLD fMRI Correlates Highly With H215O PET rCBF. *J Cereb Blood Flow Metab*. 1996; 16:755–759. [PubMed: 8784221]
39. Righini A, et al. Functional MRI: primary motor cortex localization in patients with brain tumors. *J Comput Assist Tomogr*. 1996; 20:702–708. [PubMed: 8797897]
40. Shitara H, Shinozaki T, Takagishi K, Honda M, Hanakawa T. Time course and spatial distribution of fMRI signal changes during single-pulse transcranial magnetic stimulation to the primary motor cortex. *NeuroImage*. 2011; 56(3):1469–1479. [PubMed: 21396457]
41. Smith SM, et al. Advances in functional and structural MR image analysis and implementation as FSL. *NeuroImage*. 2004; 23(Suppl 1):S208–19. [PubMed: 15501092]
42. Speck O, Hennig J, Zaitsev M. Prospective real-time slice-by-slice motion correction for fMRI in freely moving subjects. *MAGMA*. 2006; 19:55–61. [PubMed: 16779560]
43. Steger TR, Jackson EF. Real-time motion detection of functional MRI data. *J Appl Clin Med Phys*. 2004; 5:64–70. [PubMed: 15738913]
44. Stern JM, et al. Functional imaging of sleep vertex sharp transients. *Clin Neurophysiol*. 2011; 22(7):1382–1386. [PubMed: 21310653]
45. Szaflarski JP, et al. Comprehensive presurgical functional MRI language evaluation in adult patients with epilepsy. *Epilepsy Behav*. 2008; 12(1):74–83. [PubMed: 17964221]
46. Thesen S, Heid O, Mueller E, Schad LR. Prospective acquisition correction for head motion with image-based tracking for real-time fMRI. *Magn Reson Med*. 2000; 44:457–465. [PubMed: 10975899]
47. Umenyama S. Least-squares estimation of transformation parameters between two point patterns. *IEEE Trans Pattern Anal Mach Intell*. 1991; 13:376–380.
48. van der Kouwe AJW, Benner T, Dale AM. Real-time rigid body motion correction and shimming using cloverleaf navigators. *Magn Reson Med*. 2006; 56:1019–1032. [PubMed: 17029223]
49. Voyvodic JT, Petrella JR, Friedman AH. FMRI activation mapping as a percentage of local excitation: Consistent presurgical motor maps without threshold adjustment. *J Magn Reson Imag*. 2009; 29:751.
50. Vulliemoz S, et al. Simultaneous intracranial EEG and fMRI of interictal epileptic discharges in humans. *Neuroimage*. 2011; 54(1):182–190. [PubMed: 20708083]
51. Ward HA, et al. Prospective multiaxial motion correction for fMRI. *Magn Reson Med*. 2000; 43:459–469. [PubMed: 10725890]

52. Welch EB, Manduca A, Grimm RC, Ward HA, Jack CR Jr. Spherical navigator echoes for full 3D rigid body motion measurement in MRI. *Magn Reson Med.* 2002; 47:32–41. [PubMed: 11754440]
53. White N, et al. PROMO: Real-time prospective motion correction in MRI using image-based tracking. *Magn Reson Med.* 2010; 63:91–105. [PubMed: 20027635]
54. Zaitsev M, Dold C, Sakas G, Hennig J, Speck O. Magnetic resonance imaging of freely moving objects: prospective real-time motion correction using an external optical motion tracking system. *NeuroImage.* 2006; 31:1038–1050. [PubMed: 16600642]
55. Zhang Q, et al. Active MR guidance of interventional devices with target-navigation. *Magn Reson Med.* 2000; 44:56–65. [PubMed: 10893522]

### Highlights

First group level analysis of prospective motion correction in fMRI

Active marker system significantly increases the quality of fMRI data

Active marker system increases group activation cluster sizes by at least 10%

System significantly increases statistical power in areas of activation

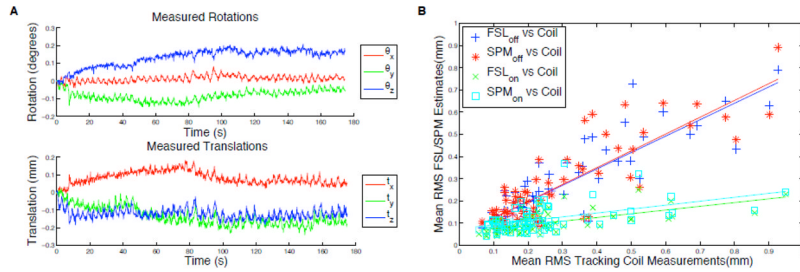


**Figure 1.**

A. Motion plot (rotations and translations) as measured by the PRAMMO tracking coils (one measurement per image slice) for a single scan. Rotations and translations in x (Red), y (Blue), and z (Green) planes are shown. Note the respiratory oscillations in the motion data.

B. Motion Estimate Correlations. Points are the mean root mean squared (rms) deviations from the middle volume of each scan session across all subjects. “Off” denotes scans in which PRAMMO was not applied but tracking coil locations (Coil) were still logged. “On” denotes scans in which PRAMMO was on and applied. FSL “off” and SPM “off” vs. the PRAMMO tracking coil show similar correlations. FSL “on” and SPM “on” vs. the PRAMMO tracking coil exhibit non-linear correlation patterns indicating that in the PRAMMO “on” case, subject motion has been corrected to a point where FSL and SPM are modeling noise image time series.

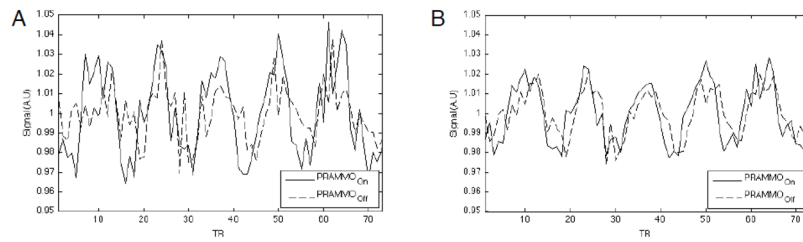


**Figure 2.**

Single voxel (MNI coordinates: 16, -90, -2 mm) time series of unsmoothed(A) and smoothed data(B) for a single subject and run, showing both PRAMMO “on” and PRAMMO “off” data for the Flickering Checkerboard experiment. The voxel was chosen as the max z-score for Group Level Mixed Effects results for both PRAMMO “on”(z=6.19) and PRAMMO “off”(z=6.31) with no retrospective correction.

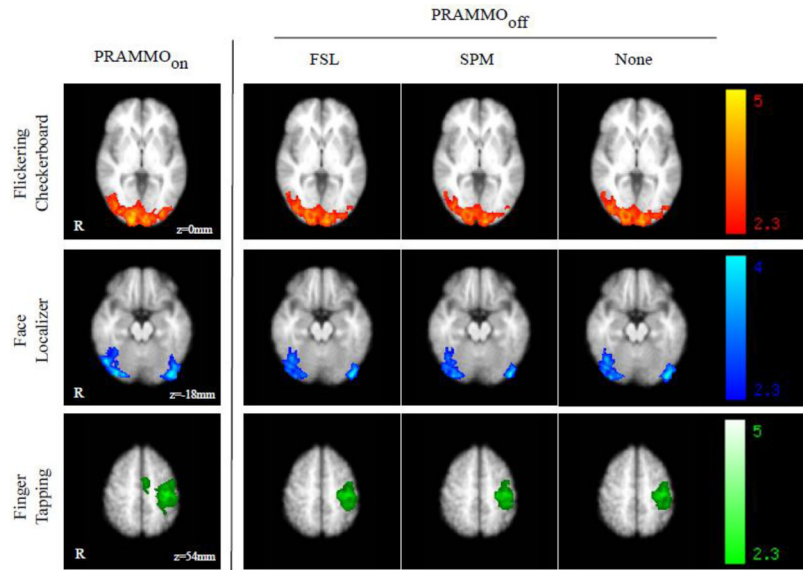


**Figure 3.** Statistical z-score maps for the fMRI group analysis ( $n=12$ ) of each motion correction technique (columns) applied to all 3 experimental paradigms (rows). The first column shows the group results when the data was acquired with PRAMMO “on”. The second, third and fourth columns are the results from the data acquired without PRAMMO (PRAMMO “off”). Columns 2 and 3 are retrospectively realigned using FSL and SPM algorithms respectively. No motion correction algorithm is applied to the data in the last column. Statistical maps are cluster thresholded by  $\geq 2.3$  and cluster significance  $p < .05$ . Color bars are provided to show scales of activation.

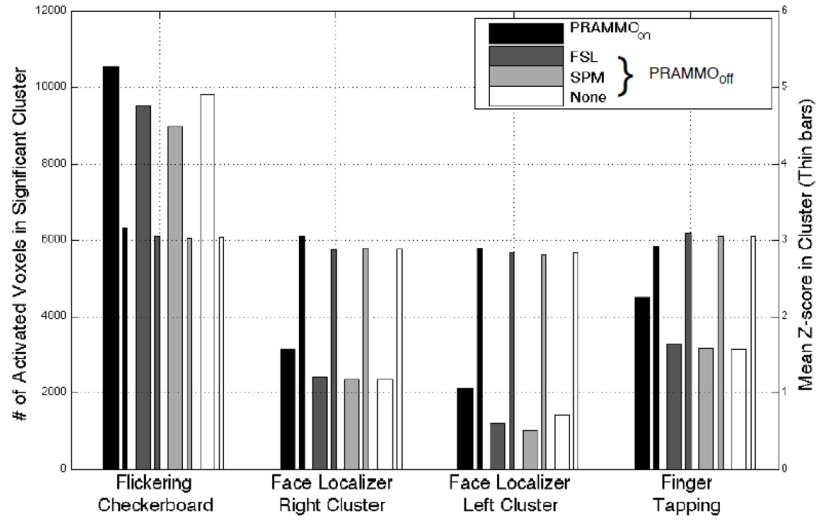


**Figure 4.** Cluster Size and Mean z-score bar plots. Quantitative analysis of the group level (n=12) cluster activation sizes and mean z-scores within the cluster for all 3 paradigms and the bilateral clusters for the Face Localizer experiment. The wide bars represent the number of activated voxels in the significant clusters, while the thin bars represent the mean z-score within that cluster. In all experiments, PRAMMO provided larger significant clusters compared to retrospective motion correction techniques or to no correction.

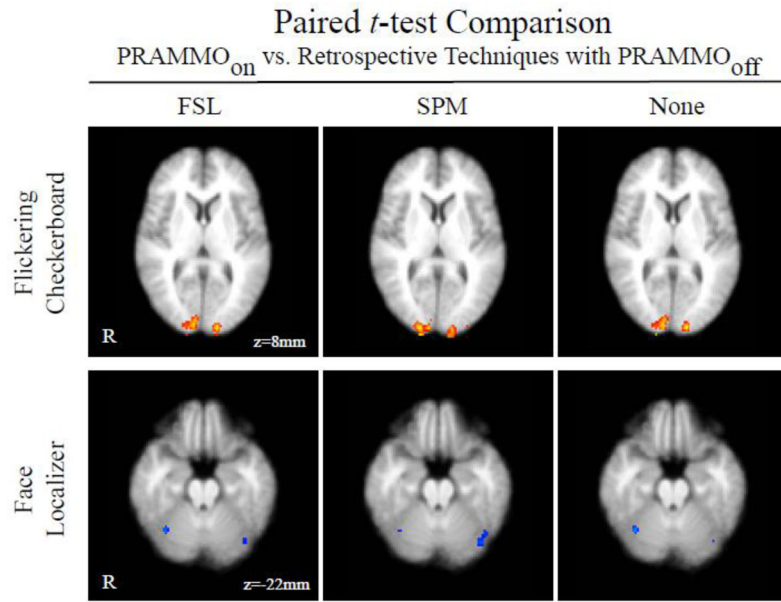


**Figure 5.** Paired *t*-test comparing PRAMMO “on” vs. Retrospective Techniques. The first column shows z-scores of a group paired *t*-test showing the areas of increased statistical power for PRAMMO “on” data compared to PRAMMO “off” data that has been retrospectively aligned using FSL’s MCFLIRT, SPM’s *spm\_realign* algorithm, and No Retrospective Correction for Flickering Checkerboard and Face Localizer paradigms (rows). Maps are thresholded at  $p < 0.001$  (uncorrected). Results for Finger Tapping paradigm did not pass threshold and therefore are not shown.

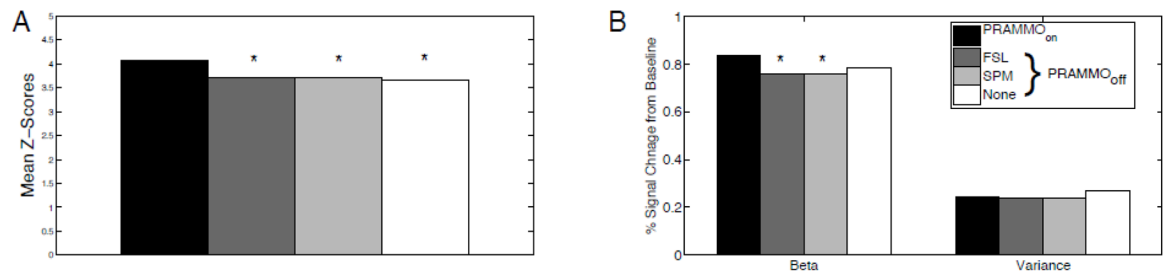


**Figure 6.**

Region of Interest Analysis Bar plots. A. Mean subject level ROI z-score across all subjects and experiments. Each bar represents the mean of 36 (12 subjects x 3 experiments) mean z-scores. B. Percent signal changes from baseline for the betas and variances across all subjects and experiments. A “\*” indicates significant difference from PRAMMO at the  $p < 0.05$  level, Wilcoxon Paired Signed Rank Test.